

# Synthesis and Phase Relationships between Smectite and Low-silica Zeolites

メタデータ	言語: eng 出版者: 公開日: 2022-12-05 キーワード (Ja): キーワード (En): 作成者: メールアドレス: 所属:
URL	<a href="https://doi.org/10.24517/00010386">https://doi.org/10.24517/00010386</a>

This work is licensed under a Creative Commons Attribution-NonCommercial-ShareAlike 3.0 International License.



## Synthesis and Phase Relationships between Smectite and Low-silica Zeolites

TAKAKO NAGASE<sup>a,\*</sup> and KAZUE TAZAKI<sup>b</sup>

<sup>a</sup> AIST, Tohoku, 4-2-1, Nigatake, Miyagino-ku, Sendai 983-8551, Japan

<sup>b</sup> Kanazawa University, Kakuma-machi, Kanazawa, Ishikawa, Japan

(Received August 21, 2005. Accepted December 28, 2005)

### ABSTRACT

Low-silica zeolite samples and smectite were hydrothermally synthesized from Si-Al hydrous oxides. The synthesized zeolite phases changed to structures having lower Si/Al ratio with increases in the amount of NaOH in the slurry, and time of hydrothermal treatment. When tetraethyl ammonium hydroxide (TEAOH) was added instead of NaOH, ammonium smectite was produced without zeolite. SEM and TEM images suggested that crystallization occurred at the solid-liquid interface. Upon addition of NaOH ( $\text{Na/Si} < 0.2$ ) to the smectite, zeolite nucleation was observed on the surface of the clay film. The zeolite phase changes depended on the dissolution of the solid phase and the resultant change in composition of the liquid phase. The observed phase relationships agreed with the calculated formation free energies and solubilities. Thus, low-silica zeolite formation under hydrothermal conditions was strongly affected by the composition and concentration of the solution. The phase relationships based on solubility curves, can be used to control the synthesis of metastable aluminous silicates and can be applied to the design of some industrial materials such as zeolite membranes and molecular sieves using hydrophilic low-silica zeolites and smectites.

Key words: Smectite, Hydrothermal synthesis, Low-silica zeolite, Phase relationships, SEM, TEM

### INTRODUCTION

The hydrous silicates, zeolite and smectite have been studied. The hydrous silicates, zeolite and smectite, have been studied and synthesized for industrial applications such as molecular sieves, ionic exchangers, and catalysis. Smectite has a 2:1 layer structure<sup>1)</sup>, whereas zeolite has a 3D structure consisting of a Si-O-Al framework with a water-containing cage. There are more than 160 framework types of zeolite<sup>2)</sup>, and the relationship between these structures and their crystallization mechanism (i.e., how and which parameters control the crystallization) is still a significant theme for synthesis because they are thermodynamically metastable minerals.

Previously, Pal-Borbely et al.<sup>3)</sup> reported on the hydrothermal synthesis of high-silica MFI and MEL-type zeolites by recrystallization of aluminosilicic acid derivatives retaining the framework topology of a layer polysilicate. More recently, Moloy et al.<sup>4)</sup> calculated the internal surface area of 17 high-silica zeolite framework types using Cerius molecular simulation software, and they found that the internal surface area and experimental value of formation

enthalpies had a linear relationship. They also noted that the internal surface area was not strongly dependent on the specific nature of the framework. Mosser-Ruck and Cathelineau<sup>5)</sup> performed the transformation of smectite to zeolite, and reported Na- and Ca-smectites were partly replaced by merlinoite (MER:  $\text{K}_2\text{Al}_2\text{Si}_5\text{O}_{14}\cdot 5\text{H}_2\text{O}$ ) in the presence of 1 M  $\text{K}_2\text{CO}_3$ . MER has a compositional similarity to Phillipsite (PHI:  $(\text{Na},\text{K})_2\text{Al}_2\text{Si}_5\text{O}_{14}\cdot 5\text{H}_2\text{O}$ ) through cation exchange of K by Na, and a structural similarity in the [100] and [001] directions<sup>2)</sup>. Donahoe and Liou<sup>6)</sup> discussed the crystallization mechanism of MER and PHI, and concluded that it depended on the Si/Al ratio, controlled by the pH of the K-H<sub>2</sub>O solution. Skofteland et al.<sup>7)</sup> hydrothermally synthesized K-MER and noted that a H-bound K-H<sub>2</sub>O network acts as an inorganic template for the crystallization of MER. Under the condition of solid state syntheses, Ikeda et al.<sup>8)</sup> successfully synthesized a new framework type (CDO) of zeolite named CDS-1 by a dehydration technique using the specific feature of a layer silicate.

Recently, we synthesized low-silica zeolites from a hydrous oxide solution in the ratio of Si-Al-Co = 1-0.15-0.05, respectively, and reported that the synthesized phases were changed in the sequence of mordenite (MOR: NaAl

$\text{Si}_5\text{O}_{12}\cdot 3\text{H}_2\text{O}$ ), phillipsite, analcime (ANA:  $\text{NaAlSi}_2\text{O}_6\cdot \text{H}_2\text{O}$ ), and sodalite (SOD:  $\text{Na}_3\text{Al}_3\text{Si}_3\text{O}_4\cdot 4\text{H}_2\text{O}$ ), depending on the time of hydrothermal treatment and the concentration of NaOH in the initial slurry<sup>9</sup>, and the pore size in the structure seemed to decrease with the reaction. In this study, the structural change of zeolite with time of hydrothermal treatment was verified by electron microscopy, and the synthesis of zeolite and smectite from a hydrous oxide by addition of different alkali elements were performed to evaluate their phase relationships.

## EXPERIMENTAL MATERIALS AND METHODS

### Sample preparation

To evaluate the crystallization process of smectite at varying temperatures and times, the smectite mineral hectorite ( $\text{Na}_{0.3}(\text{Mg}_{1.7}, \text{Li}_{0.3})\text{Si}_4\text{O}_{10}(\text{OH})_2\cdot n\text{H}_2\text{O}$ ), was synthesized by the method of Torii<sup>10</sup> from a hydrous oxide solution with a Si-Mg ratio of 4-1.7, respectively. The NaOH and LiOH were added to the Si-Mg hydrous oxide solution to make a homogeneous slurry at pH of 10. The slurry was hydrothermally treated at 150-400 °C for 2 h in an autoclave with stirring. The slurry was also treated hydrothermally at 200 °C for 0.5-24 h without stirring in a Teflon container set inside a stainless steel bottle. To study the dissolution and recrystallization mechanism of smectite, 0.005 - 0.2 % solution of SWN (synthetic hectorite, COOP Chemical Co. Ltd.) was used as a starting material. Lithium hydroxide (LiOH) was added to adjust the pH to 10. The hectorite solution was flowing continuously at the rate of 0.5 mL/min through the SUS316 column (1.6 mm inside diameter x 10 m length) heated to 375 °C in an oven under 25 MPa pressure. The products were dispersed in water and observed by transmission electron microscopy (TEM). Si-Al hydrous oxides were also prepared as starting materials for synthesis of di-octahedral smectite ( $\text{M}_x\text{Al}_2(\text{Si}_{4-x}, \text{Al}_x)\text{O}_{10}(\text{OH})_2\cdot n\text{H}_2\text{O}$ ,  $\text{M} = \text{Na}^+, \text{K}^+, \text{NH}_4^+, 0 < x < 0.6$ ) and low-silica zeolites. To evaluate the effect of Na-content on the crystallization of zeolites and smectite, colloidal silica of low Na content was used for the preparation. The colloidal silica, SI30 ( $\text{SiO}_2$  30%,  $\text{Na}_2\text{O} < 0.5\%$ , Shokubaikasei Co.) was mixed with  $\text{AlCl}_3\cdot 6\text{H}_2\text{O}$ , and then co-precipitated by titration with  $\text{NH}_4\text{OH}$ . For the synthesis of di-octahedral smectite and zeolite, NaOH, KOH, and tetraethyl ammonium hydroxide (TEAOH:  $(\text{C}_2\text{H}_5)_4\text{NOH}$ ) were added to the Si-Al hydrous oxide solution to in the pH range of 12-14. The slurry was hydrothermally treated in the Teflon container inside a stainless steel bottle at 150-200 °C without stirring. After the treatment, the bottle was quenched by water, and the products were filtrated and dried at 60 °C.

### Instrumental

Identification of the minerals was obtained from a Rigaku X-ray diffractometer (XRD) RINT2100 with  $\text{Cu K}\alpha$  radiation, set at 20 mA and 40 kV. Chemical analysis of the reaction products were carried out using a S-800 HITACHI field emission type scanning electron microscope

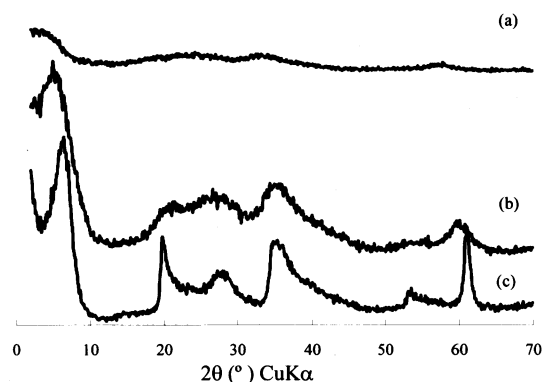


Fig. 1 XRD patterns of a Si-Mg hydrous oxide (a) and hectorite hydrothermally synthesized at 200 °C for 0.5 h (b) and 2 h (c).

(FE-SEM) equipped with an EMAXenergy EX-320 Horiba energy dispersive X-ray spectrometer (EDX), as well as a JEOL JEM2000EXII TEM.

## RESULTS

### Observation of Si-Mg-Li trioctahedral smectite (hectorite)

The XRD pattern of the synthesized Si-Mg hydrous oxide (Fig. 1) showed a structural similarity to smectite in the ab plane as described by Torii<sup>10</sup>. In the TEM images of the products following hydrothermal treatment at 150-200 °C for 2h, the particle size was observed to be about 10-15 nm in the ab plane, and not appreciably different from the initial Si-Mg hydrous oxide. A porous lump of particles is shown in Fig. 2a, which is similar to the "primitive clay" reported by Tazaki et al.<sup>11</sup> in the crystallization from a glass. The

**Table 1** Hydrothermal synthesis of low-silica zeolites from Si-Al hydrous oxide solution at 200 °C

Run No	Condition of Hydrothermal synthesis <sup>a</sup>				Products identified by XRD
	Hydrous oxide Si/Al ratio	added alkali species	alkali/Si ratio	time (h)	
1	2	TEAOH	0.5	48	smectite(low crystallized)
2				72	
3	6.7	NaOH	0.5	48	MOR
4				124	
5				41	
6	5	NaOH	0.5	46	MOR+PHI
7				48	
8				4	
9				4	
10	2	NaOH	1	4	ANA
11				48	
12	1	NaOH	5	24	SOD+JBW
13				46	
14	2	KOH	1	24	MER
15				24	
16				24	

MOR: mordenite, ANA: analcime, PHI: phillipsite, SOD: sodalite, JBW: Na- zeolite J, MER: merlinoite

<sup>a</sup>Concentration of the hydrous oxide solution was [Si] 2 mol/L.

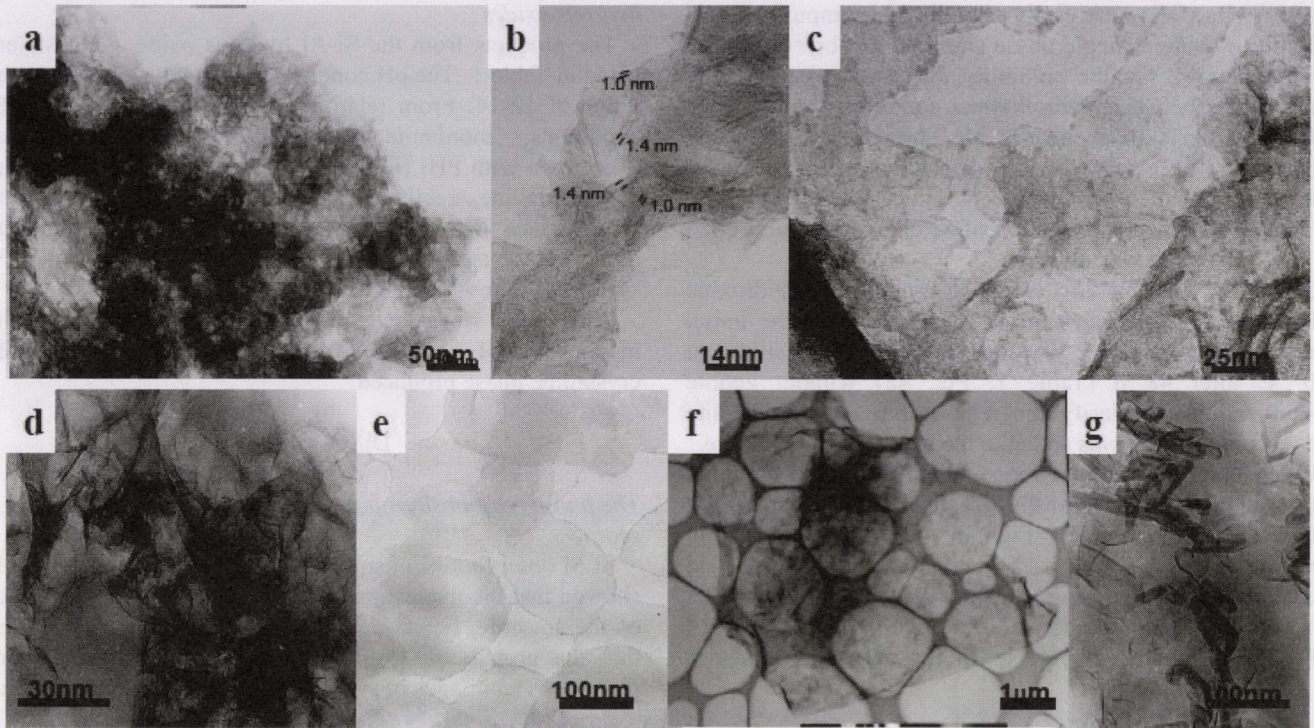


Fig. 2 TEM images of synthetic hectorite (a - f) and serpentine (g) in the Na-Si-Mg system.

- (a) Poorly-crystallized hectorite hydrothermally synthesized at 150 °C for 2h from the Si-Mg hydrous oxide. The porous lump of small particles is similar to "primitive clay" in the early stages of crystallization from glass.
- (b) The lattice image of the product synthesized at 200 °C for 30 min having the same texture with the products of (a). The thickness of the layer was irregular and larger than that of smectite.
- (c) The products synthesized at 200 °C for 24 h shows a clay film.
- (d) The products synthesized at 290 °C for 2h shows a large film of hectorite and small reminders of Si-Mg hydrous oxide.
- (e) The submicron size particles of hectorite synthesized at 400 °C for 2h.
- (f) The recrystallized large hectorite film obtained by hydrothermal treatment of 0.2 wt% of small synthetic hectorite solution at 375 °C, 25 MPa in flow system.
- (g) The serpentine particles obtained by hydrothermal treatment of 0.05 wt% of small synthetic hectorite solution at 375 °C, 25 MPa in flow system.

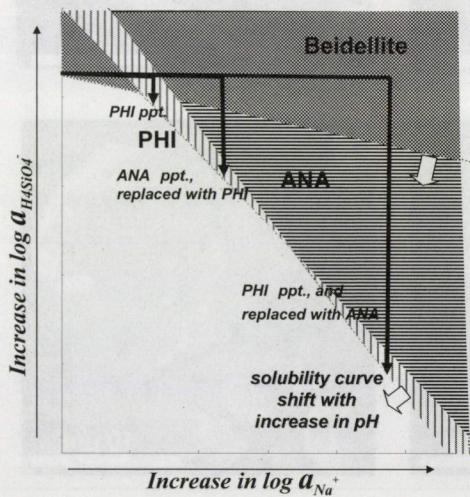


Fig. 3 Schematic of phase relationship between beidellite and the zeolites based on the solubility curves.<sup>12)</sup>

ANA:  $\text{NaAlSi}_2\text{O}_6 \cdot \text{H}_2\text{O}$ , ( $\Delta G_f = -3080 \text{ kJ/mol}$ )

PHI:  $\text{Na}_2\text{Al}_2\text{Si}_5\text{O}_{14} \cdot 5\text{H}_2\text{O}$ , ( $\Delta G_f = -7628 \text{ kJ/mol}$ )

Beidellite:  $\text{Na}_{0.3}\text{Al}_{1.3}\text{Si}_{3.7}\text{O}_{10}(\text{OH})_2$ , ( $\Delta G_f = -2072 \text{ kJ/mol}$ )

thickness of each particle was about 1.4 nm and thicker than that of well-crystallized smectite. After treatment at 200 °C for 24 h, the thickness of the layer structure became uniform at 1.0 nm, and the particles showed film-like features (Fig. 2b, 2c). At temperatures higher than 250 °C, 30~200 nm smectite particles were observed with the remaining particles of Si-Mg hydrous oxide dissolved (Fig. 2d, 2e). In the recrystallization test of hectorite, initial hectorite particles were almost resolved at temperatures over 375 °C. When the initial concentration was higher than 0.2 wt%, large smectite films were obtained (Fig. 2f), however, when the initial concentration was low, hectorite did not recrystallize and serpentine crystallized instead of smectite (Fig. 2g). Thus, under conditions of low temperature, dissolution of the initial Si-Mg hydrous oxide was so slow that the crystallization of smectite occurred from the solid-liquid interface epitaxially on the remaining hydrous oxide structure.

*Phase relationships between dioctahedral smectite and zeolite – effect of pH and addition of NaOH*

In the Si-Al system, optimum conditions for syntheses of di-octahedral smectite were more restricted in comparison to

that for hectorite, because PHI, ANA, and paragonite ( $\text{NaAl}_3\text{Si}_3\text{O}_{10}(\text{OH})_2$ ) are easily crystallized as impurities. It is difficult to obtain a single phase smectite, as observed in the Si-Fe system<sup>12</sup>. On the solubility diagram<sup>13</sup> (Fig. 3), the relationships between hydrothermal conditions and relative stability of crystalline phases are shown. The high pH condition is necessary for the crystallization of smectite, however, an increase in Na content induces the precipitation of zeolites. Thus, crystallization of zeolite can be controlled on Na/Si ratio and pH condition.

Upon an addition of tetraethyl ammonium hydroxide (TEAOH) or  $\text{NH}_4\text{OH}$  instead of NaOH to adjust the initial slurry to a pH of 12-13, smectite (beidellite) crystallized at 200 °C after 48 h (Table 1, Fig. 4a) without zeolite crystallization. To clarify the relationship between zeolite and smectite, NaOH was added to the synthesized beidellite.

When  $\text{Na/Si} < 0.2$  (molar ratio), small particles of zeolite nucleated on the surface of the smectite film-like particles at 200 °C after 30 minutes (Fig. 4b, 4c). Then, after 2 h, herschellite (Na-CHA:  $\text{NaAlSi}_2\text{O}_6 \cdot 3\text{H}_2\text{O}$ ) crystallized and was replaced by PHI (Fig. 4d, 4e). When  $\text{Na/Si} = 0.625$ , smectite entirely dissolved at 200 °C within 2 h, and ANA and PHI crystallized. Fig. 4e shows that ANA was replaced by PHI.

#### *The phase relationships of the low-silica zeolite from Si-Al hydrous oxides*

The products from the Si-Al hydrous oxide synthesis are listed in Table 1. The pH conditions for syntheses were in the range of 12-14. From relatively high Si/Al and low Na/Si conditions, mordenite (MOR) crystallized and was overgrown with PHI (Fig. 5d-f). Thus, in the presence of Na, the crystalline zeolite phases changed regularly in the sequence of MOR, PHI, ANA, to SOD similar to that reported by Nagase et al.<sup>9, 12</sup> for the Si-Al-Co, and Si-Al-Fe system with or without TEAOH.

When KOH was added to the hydrous oxide solution in the molar ratio of K/Si of 0.05 to 0.5, MER was the only crystalline phase produced.

## DISCUSSION

#### *The phase relationships between smectite and low-silica zeolite*

SEM observations of smectite following addition of NaOH showed that the nucleation of zeolite occurred on the surface of the smectite, however, the SEM images (Fig. 4) suggest that the growth of zeolite was due to the dissolution of smectite. The images of synthetic PHI obtained from hydrous

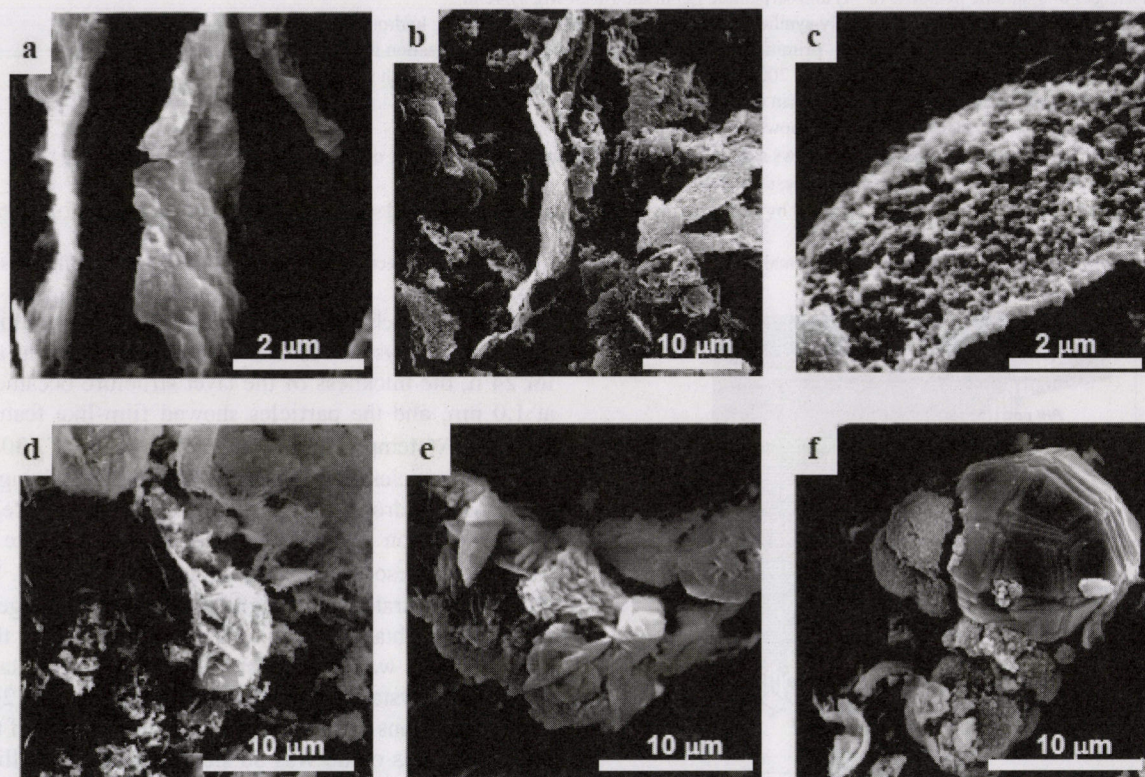


Fig. 4 SEM images of beidellite hydrothermally synthesized from Si-Al hydrous oxide at 200 °C after 48 h (a) and zeolites obtained by the treatment of the beidellite with NaOH solution at 200 °C under condition of  $\text{Na/Si} < 0.2$  for 30 min (b, c), 2 h (d, e) and the condition of  $\text{Na/Si} = 0.625$  for 2 h (f). Upon addition of NaOH, nucleation of zeolite was observed on the surface of the smectite films. After 2h, herschellite grew and replaced by phillipsite. With additional NaOH, beidellite entirely dissolved and analcime crystallized and was replaced by phillipsite.

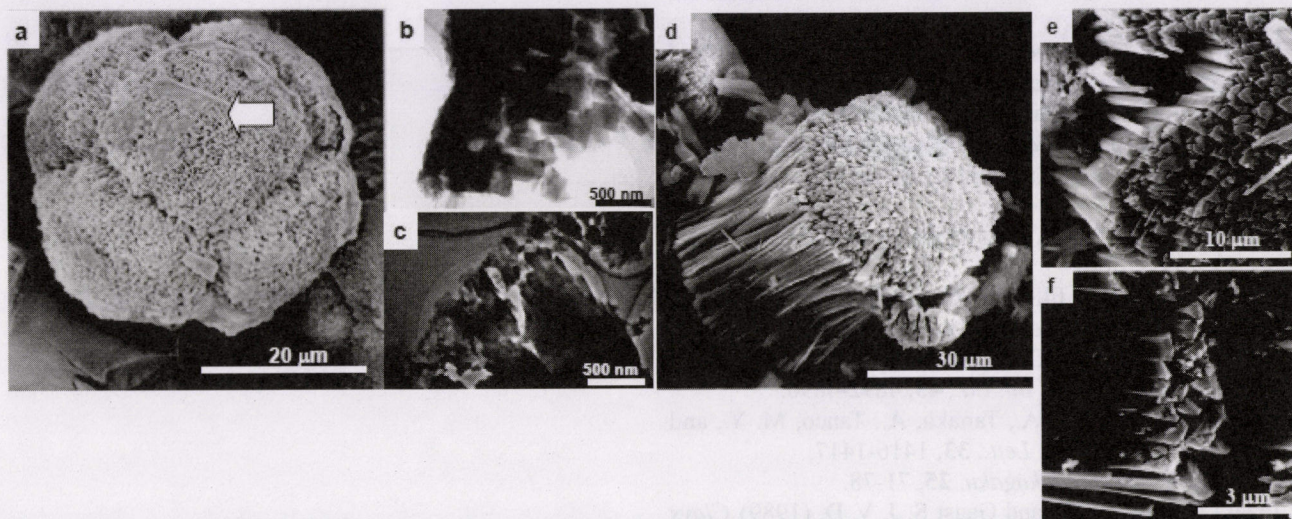


Fig. 5 SEM and TEM images of PHI polycrystals synthesized from various hydrous oxide solutions.

- (a) A spherical particle of PHI synthesized at 150 °C for 4 h from the 2 mol/L [Si] of hydrous oxide solution ( $\text{Na}_{2.5}\text{Si}_4\text{Al}_{1.7}\text{Fe}_{0.3}$ ) with 1 mol/L of TEAOH.<sup>12)</sup> The skin-like layer on the particle is observed (indicated with an arrow).
- (b) Cross section of the spherical particle of PHI.  
The skin-like layer on the particle in (a) consists of a layer silicate and fills the interparticle space of PHI.
- (c) The image suggests that small PHI crystals grew from surface of the spherule to outer side, and suggests presence of highly concentrated solution surrounded the PHI crystals during the synthesis.
- (d) Overgrowth of PHI on the fibrous MOR synthesized at 200 °C for 124 h from the hydrous oxide solution of Si/Al=6.7 listed in Table 1.
- (e) The surface of the MOR particle overgrown with PHI.
- (f) Enlarged image of the interface between MOR and PHI.

oxide solutions under low NaOH concentrations and short reaction times showed that the particles were hollow spherules or had cores of low-crystallinity. The spherules were surrounded by well-crystalline particles of PHI growing outward from the rim of the spherules (Fig. 5). In Fig. 5a, the surfaces of the spherical particles were partly covered with skin-like layers. Under the TEM, it was observed that a layer silicate precipitated and filled interparticle spaces of the PHI crystallites (Fig.5b), which suggests that a highly concentrated solution surrounded the PHI crystals during growth. These observations imply that the crystallization of the zeolite phase took place at the solid-liquid interface and was controlled by the dissolution of the solid phase.

#### Structural relationships between zeolite phases

According to Baerlocher et al.<sup>2)</sup>, it is difficult to find a structural similarity between the Si-O frameworks of MOR, PHI and ANA. To evaluate how structural changes of zeolite phases are controlled, the formation free energies of some zeolites calculated by the polymer free model<sup>14)</sup> are compared. The calculated values were -3080 kJ/mol for ANA, -3558 kJ/mol for Na-CHA, -3814 kJ/mol for PHI (the value for the half unit), and -6093 kJ/mol for MOR. In the polymer model method, the framework types of the zeolites were not considered and the value was simply dependent on the chemical composition. The resulting value increased with a decrease in Si/Al ratio and number of coordinated waters in the ideal formula of each zeolite, and the calculated values almost coincided with the sequence of phase changes recognized in the syntheses. Thus, the zeolite phases transformed to be more thermodynamically stable via

dissolution and recrystallization.

According to Mattigod and McGrail<sup>14)</sup>, the formation free energy of MER is lower compared to that of PHI and higher relative to ANA. In this study, MER could not be obtained without addition of KOH, whereas K is exchangeable with Na in synthesized MER, which demonstrates that the alkaline cations determine the crystalline phases as predicted by Skofteland et al.<sup>7)</sup>. Thus, topological difference in polymorphs of zeolite should be dependent on the alkali cation species added for the synthesis.

#### CONCLUSION

The phase relationships observed in the hydrothermal syntheses of smectite and low-silica zeolites from hydrous oxide solutions were strongly affected by the compositional change of the solution during the reaction with solid phases, and differences in the solubility of each phase. The methods to synthesize hydrophilic low-silica zeolites and smectites can be applied to synthesize industrial materials such as zeolite membranes, and molecular sieves using hydrophilic low-silica zeolites and smectites.

#### REFERENCES

- 1) Güven, N. (1988) *Smectites, Reviews in Mineralogy*, **19**, Chapter 13, Mineral. Soc. Amer., Washington, DC, 497-552.
- 2) Baerlocher, Ch., Meier, W.M., and Olson, D.H.(2001) *Atlas of Zeolite Framework Types*, 5th Edit., Structure

Commission of the International Zeolite Association,  
Elsevier, Amsterdam.

- 3) Pal-Borbely, G., Beyer, H. K., Kiyozumi, Y., and Mizukami, F. (1997) *Micropor. Mater.*, **11**, 45-51.
- 4) Moloy, E.C., Davila, L.P., Shackelford, J.F., and Navrotsky, A. (2002) *Micropor. Mesopor. Mater.*, **54**, 1-13.
- 5) Mosser-Ruck R. and Cathelineau M. (2004) *Appl. Clay. Sci.*, **26**, 259-273.
- 6) Donahoe, R.J. and Liou, J.G. (1985) *Geochim. Cosmochim. Acta*, **49**, 2349-2360
- 7) Skofterland, B. M., Ellestad, O. E. and Lillerud, K. P. (2001) *Micropor. Mesopor. Mater.*, **43**, 61-71.
- 8) Ikeda, T., Akiyama, Y., Oumi, Y., Kawai, A. and Mizukami, F. (2004) *Angew. Chem., Int. Ed.*, **43**, 4892-4896.
- 9) Nagase, T., Chatterjee, A., Tanaka, A., Tanco, M. Y., and Tazaki, K. (2004) *Chem. Lett.*, **33**, 1416-1417.
- 10) Torii, K. (1985) *Nendokagaku*, **25**, 71-78.
- 11) Tazaki K, Fyfe W. S., and Gaast S. J. V. D. (1989) *Clays and Clay Minerals*, **37**, 348-354.
- 12) Nagase, T. (2001) Abstract of chemical society of JAPAN.
- 13) Nagase, T., Ebina, T., Iwasaki, T., Hayashi, H., Onodera, Y. and Dutta, N. C. (1999) *Chem. Lett.*, 313-314.
- 14) Mattigod, S.V., and McGrail, B.P. (1999) *Micropor. Mesopor. Mater.*, **27**, 41-47.